South Dakota State University

Open PRAIRIE: Open Public Research Access Institutional Repository and Information Exchange

Electronic Theses and Dissertations

2018

Analysis of 3D Printed Cylindrical Members

Salvador Caballero
South Dakota State University

Follow this and additional works at: https://openprairie.sdstate.edu/etd

Part of the Civil and Environmental Engineering Commons, and the Materials Science and Engineering Commons

Recommended Citation

Caballero, Salvador, "Analysis of 3D Printed Cylindrical Members" (2018). *Electronic Theses and Dissertations*. 2694.
https://openprairie.sdstate.edu/etd/2694

This Thesis - Open Access is brought to you for free and open access by Open PRAIRIE: Open Public Research Access Institutional Repository and Information Exchange. It has been accepted for inclusion in Electronic Theses and Dissertations by an authorized administrator of Open PRAIRIE: Open Public Research Access Institutional Repository and Information Exchange. For more information, please contact michael.biondo@sdstate.edu.

ANALYSIS OF 3D PRINTED CYLINDRICAL MEMBERS

BY

SALVADOR CABALLERO

A thesis submitted in partial fulfillment of the requirements for the

Master of Science

Major in Civil Engineering

South Dakota State University

2018

ANALYSIS OF 3D PRINTED CYLINDRICAL MEMBERS

SALVADOR CABALLERO

This thesis is approved as a creditable and independent investigation by a candidate for the Master of Science in Civil Engineering degree and is acceptable for meeting the thesis requirements for this degree. Acceptance of this does not imply that the conclusions reached by the candidate are necessarily the conclusion of the major department.

Suzette Burckhard, Ph.D.
Advisor — Date

Nadim Wehbe, Ph.D.
Head, Department of Civil and Environmental Engineering — Date

Dean, Graduate School — Date

ACKNOWLEDGEMENTS

I would like to acknowledge the National Science Foundation (NSF) 1642037, Oglala Lakota College (OLC), South Dakota State University (SDSU), and South Dakota School of Mines and Technology (SDSMT) Pre-Engineering Education Collaborative-II (OSSPEEC-II) for supporting and funding this research. I am indebted to Dr. Suzette Burckhard, OSSPEEC-II interns at SDSU; Calvin Wampol, Yazen Hindien, Jamie Van Zee, and Katrina Burckhard; and Dr. Todd Letcher for their technical support with help in my research. I would also like to thank the professors and instructors at SDSU for providing me with the knowledge and skills I have gained throughout my career.

TABLE OF CONTENT

ABBREVIATIONS vi

LIST OF FIGURES vii

LIST OF TABLES x

ABSTRACT xi

Chapter 1: Introduction 1

Chapter 2: Literature Review 3

2.1 History of 3D Printing 3
2.2 Applications of 3D Printing 4
2.3 3D Printing in Civil Engineering 5
2.4 Columns 5
2.5 Polylactic Acid (PLA) 6
2.6 Thin Wall Pressure Vessel Theory 6

Chapter 3: Materials and Methods 8

3.1 Sample Identification 11
3.2 First Design 11
3.3 Compacting. 17
3.4 Compressive Testing. 20
3.5 Analyzing the Data 21
3.6 Quality Control 23

Chapter 4: Research Results and Discussion 24

4.1 First Design 24
4.2 Second Design 29
4.3 Compare & Contrast 37
4.4 Failure Mechanisms 41

Conclusion 48

Future Recommendations and OLC projects 49

References 50

Appendix A: Equations 52

ABBREVIATIONS

A = Area

d_o = Sample outer diameter

d_i = Sample inner diameter

F = Applied load

S = Sand filled cylinder

h = Sample height

n = number of observations

NS = Hollow cylinder

r = Sample radius

RNS = Random Z seam hollow cylinder

RS = Random Z seam sand filled cylinder

s = Standard deviation

t = Sample thickness

x = value of a single observation

X = mean value of the set of observations

σ_c = Circumferential (hoop) stress

σ_l = Longitudinal (axial) stress

σ_r = Radial stress

LIST OF FIGURES

Figure 2.6.1. Stresses along a cylinder pressure vessel acted by the pressure inside (P) (Pizzo,n.d.).……..…….……...7

Figure 2.6.2. Cross section of stresses along a cylinder pressure vessel. σ_h represents the hoop stress while σ_L represents the longitudinal stress acting on the wall of the pressure vessel. The thickness (t) and length (L) of the cylinder are also represented (Patel, 2016). . …….…….……..7

Figure 3.1. This figure represents the axial load, F, distributing the sand inside the cylinder, thus acting like a pressure vessel.……..... 10

Figure 3.2. Design process…….……..… 10

Figure 3.2.1. Dimensions for the cylinder height of 4.5 inches.…….. 12

Figure 3.2.2. Dimensions for the cylinder inner diameter of 1.8 inches and thickness of 0.1 inches……..……..…….. 13

Figure 3.2.3. Drawing of end caps..……. 13

Figure 3.2.4. Dimensions for the cylinder caps with a thickness of 0.1 inches……..…. 14

Figure 3.2.5. Dimensions for the cylinder caps with an inner diameter of 1.8 inches and thickness of 0.1 inches.……..… 14

Figure 3.2.6. The location of the Nozzle and Platform in the creator pro 3D printer.…….…..... 15

Figure 3.2.7. The layer height parameters set on Flashprint……..... 16

Figure 3.2.8. The shell parameters set on Flashprint……..... 16

Figure 3.2.9. The infill parameters set on Flashprint..... 16

Figure 3.2.10. The speed parameters set on Flashprint..... 16

Figure 3.2.11. The temperature parameters set on Flashprint…….....17

Figure 3.4.1. Compressive test apparatus setup……..... 21

Figure 4.1.1. Typical force-displacement data for sand filled samples; sample S-4.

…..... 24

Figure 4.1.2. Sample S-1 with critical point; Point A……..... 25

Figure 4.1.3. Force-displacement data for sand filled samples displaying the maximum force …..... 26

Figure 4.1.4. Force-displacement data for hollow samples……..... 27

Figure 4.1.5. Location of the Z seam with respect to the sample……..... 29

Figure 4.2.1. Print preference mode for Flashprint software……..... 30

Figure 4.2.2. “Start Points” mode for randomized Z seam printing..... 31

Figure 4.2.3. Sample RS3 with the randomized Z seam print..... 32

Figure 4.2.4. Typical force-displacement data for randomized Z seam sample…….... 33

Figure 4.2.5. Force-displacement data for randomized Z seam, sand filled samples….. 34

Figure 4.2.6. Force-displacement data for randomized Z seam, hollow samples……... 35

Figure 4.3.1. Comparison of the maximum forces between all the samples…….. 38

Figure 4.3.2. Comparison of the longitudinal stresses between the Z seam present and the random Z seam……..... 39

Figure 4.3.3. Comparison of the hoop stresses between the Z seam present and the random Z seam.…..... 40

Figure 4.4.1. Failure of design 1 hollow samples…….…... 42

Figure 4.4.2. Failure of design 2 hollow samples……..…..... 43

Figure 4.4.3. Failure of design 1 and design 2 hollow samples…….....44

Figure 4.4.4. Failure of design 2 sand filled samples…….....45

Figure 4.4.5. Failure of design 1 sand filled samples…….....46

Figure 4.4.6. Failure of design 1 and design 2 sand filled samples..... .47

LIST OF TABLES

Table 3.1 Mechanical properties of PLA (Makeitfrom, 2015).....8

Table 3.2. Unimin Sand properties.....9

Table 3.3. Grain size distribution table obtained for Unimin 4030 sand.....9

Table 3.1.1 Design samples' abbreviations.....11

Table 3.3.1. Typical values of void ratio (e) provided from Das…….....18

Table 3.3.2. The different weights for the first design with sand, hollow cylinders..... 19

Table 3.3.3. The different weights for the first design with sand, with randomized location of the seam..... 19

Table 4.1.1. Maximum force each of the sand filled cylinders held..... 26

Table 4.1.2. Maximum force for each of the hollow cylinders……..... 27

Table 4.1.3. Tabulated Stresses for the cylinders with sand..... 28

Table 4.1.4. Axial Compression Stress acting on hollow cylinder…..... 28

Table 4.2.1. Maximum force for each of the randomized Z seam, sand filled cylinders..34

Table 4.2.2. Maximum force for each of the randomized Z seam, hollow cylinders..... 36

Table 4.2.3. Tabulated Stresses for the cylinders with sand with randomized Z seam.... 36

Table 4.2.4. Axial Compression Stress acting on hollow cylinder..... 36

Table 4.3.4. Comparison of Hoop Stress and Ultimate Tensile Stress……..... 41

ABSTRACT

ANALYSIS OF 3D PRINTED CYLINDRICAL MEMBERS

SALVADOR CABALLERO

2018

Compressive analysis of a structural member is the determination of the axial capacity of the member when it is undergoing a load causing the member to fail in either a buckling or a crushing mode. 3D printed plastic columns have not been characterized and analyzed yet. However, this research characterizes 3D-printed PLA columns and provides parameters for future researchers to investigate. The literature describes the different industries that utilize 3D-printing. In this research, we introduce an innovative approach to investigate the stresses produced in a 3D printed composite member, made of PLA and locally available soil. The compressive testing will determine the behavior and mechanical properties of the 3D printed structural members. The compressive properties of the structural members were analyzed by following ASTM D695 *Standard Test Method for Compressive Properties of Rigid Plastics*. Then, design improvements were done to enhance the structural members' axial capacity and overall strength. It was discovered in this research that incorporating sand inside the structural member increases the overall axial capacity of the member. The different printing parameters presented different results in the different observed stresses. The failure of the structural members resembled a crushing failure along either the seam of the print or at the individual strands.

Chapter 1: Introduction

This research is designed to provide different project parameters for Oglala Lakota College (OLC) students to investigate, and to design and characterize 3D printed structural members filled with soil. Being able to reduce the overall human plastic waste is important and be able to print using this plastic. This will help reduce the waste in the oceans and help to keep the environment cleaner. The use of locally available soil would help make these structural members cost-effective. The different stresses and the failure mechanisms were studied and observed for these structural members. These types of failure mechanisms will help understand what is critical in 3D printed design structural elements. Being able to understand the behavior of these structural members will make it easier to build large scale member which would made housing affordable in communities battling with poverty. Polylactic Acid is a thermoplastic that is cheap and affordable that is used in many 3D printing applications. A compressive test on these cylindrical structural members will be tested to determine the mechanical properties of the composite members and the behavior at its failure. These members will be analyzed and the different stresses acting on them due to the pressure inside the sand will be compared to the ultimate tensile stress of the individual strands. These members will be used as the model system to investigate the overall stresses and the failure mechanisms. The cylinder members consist of 3D printed PLA hollow cylinders and fine-grained Cohesionless soil. The samples will be tested for longitudinal stresses, and circumference stress. They will be following ASTM D695 *Standard Test Method for Compressive Properties of Rigid Plastics*. Four different samples were printed to ensure proper quality control. This research followed a cyclic design method; first an initial design was developed a design

to test, second was to reduce the data to mechanical properties, and finally to improve the design according to how the structural member behaved.

Chapter 2: Literature Review

2.1 History of 3D Printing

Three dimensional printing (3D) is the process of creating a physical 3D digital model designed in a computer aided design program, by a process of adding layer by layer of materials until the physical object is created. You can print with a variety of materials that include plastics, metals, ceramics, paper, bio materials, and food. It was in the mid to late 1980's where 3D printing started. There were 3 main 3D printing technologies known as Stereolithography (SLA), Selective Laser Sintering (SLS), and Fused Deposition Modeling (FDM). The earliest form of 3D printing was patented in 1986 by Charles (Chuck) Hull. He named it the "Stereolithography Apparatus" (SLA) which prints layer by layer. SLA is a resin 3D printing or additive manufacturing process that uses photopolymer resin that can be cured. The liquid polymer is exposed to light and a UV laser draws the cross section. This is repeated until the next layer is created and then eventually pulled out of the resin. The advantage with SLA is that they can achieve higher levels of accuracy, but lack the strength of SLS or FDM. The SLA-1 hit the market in 1988.

In 1987 Carl Deckard produced the world's first SLS machine. The SLS shoots a laser at a powder of liquid. SLS uses powdered polymer as a build material that is transferred from a container holding fresh powder. A laser scans the thin layer of powder, sintering together the powder into the desired cross section. The platform is then lowered and the next layer can be created. The process is repeated until the model is complete.

In 1990, Scott Crump filed a patent for FDM. FDM is the most popular type of printer known today. FDM works by having material melted and extruded through a nozzle to create a 3D cross section. The platform is lowered after each layer is printed and the process is repeated to produce a finished product. Different types of materials can be extruded through the nozzle; thermoplastics being the most common. Several 3D printers were built and redesigned throughout the years to improve the quality of the printing and to make them more economical to the public.

2.2 Applications of 3D Printing

3D printing has been used across various industries to produce a variety of accomplishments around the world. These industries include Architecture, automotive, education, medical, and many more. In the Architecture world, 3D printing is used to design small scale replicas of products. They are used to visualize what the final product will look like. In the automotive field, parts are being printed to produce a prototype. These prototypes can be adjusted and revamped to produce a product that is better. In the education industry, 3D printing is used to boost problem solving in schools. This allows students to design and test their creations in real life to get a better understating of how different objects behave. In the medical field, 3D printing has advanced a lot. They can be organized into tissue and organ fabrication, creating prosthetics, and implants. A process known as bioprinting is a method of using living cells or biomaterials to reproduce human tissues or organs (Ventola, 2014). Organ bioprinting is still under development, but research proves a proof of concept. 3D printed prosthetics and implants and be made to fit any type of geometry.

They can be produced from an x-ray, MRI, or CT scan into its digital form. This allows for personal customizations of prosthetics that are more cost-effective.

2.3 3D Printing in Civil Engineering

3D printing in Civil Engineering has been used through the structural field, the geotechnical field, and educational field. In the structural field large scale 3D printers and concrete are coming together to develop a 3D concrete printer capable of printing a full scale house. These types of prints can provide cheap and efficient homes with less labor. In the geotechnical field, synthetic and natural, 3D printed, fibers are being studied to be used a soil reinforcement to increase the overall strength and stiffness due to their mechanical properties (Hejazi, 2012).

2.4 Columns

Columns are a vertical structural member designed to transmit a compressive load. They are used to support ceiling/roof slab and beams and distribute out the load from them to the foundations underneath. They are typically constructed of concrete, steel, and timber, and a mix of the three. These columns can be classified based on their slenderness ratio. You either have a long column (slender) or a short column. Where the length determines how the column will fail, either by buckling or by shearing, depending on the classification on their slenderness ratio. They can also be classified based on their shape; rectangular, square, circular, polygon. They can also be classified based on the type of loading such as only axially loaded column, axial load and un-axial bending column, and axial load and biaxial bending column.

2.5 Polylactic Acid (PLA)

Polylactic Acid (PLA) is a biodegradable plastic that was first discovered back in 1932 by Wallace Carothers. It is an environmentally friendly, plant derived thermoplastic that is widely used (Polymerdatabase, 2015). Since PLA is fully biodegradable, its applications are medical friendly (Davachi, 2015). The mechanical properties make it one of the stronger polymers that is commonly used in the 3D printing industry.

2.6 Thin Wall Pressure Vessel Theory.

Pressure vessels are common in everyday life ranging from storage tanks to oil tankers to scuba diving tanks. The analysis is based off the assumption that the radius to thickness ratio is less than or equal to 10. This implies that the vessel is sufficiently thin with respect to its radius. The two most common types of vessels are cylindrical vessels and spherical vessels. As the vessel is pressurized the stresses that act on a tiny element on the vessel's shell can be split up into components that act in the longitudinal (axial) direction and the circumferential or hoop direction which can be seen in Figure 2.6.1 and Figure 2.6.2. The hoop stress tries to split the cylinder along its length while the longitudinal stress tries to blow the ends off.

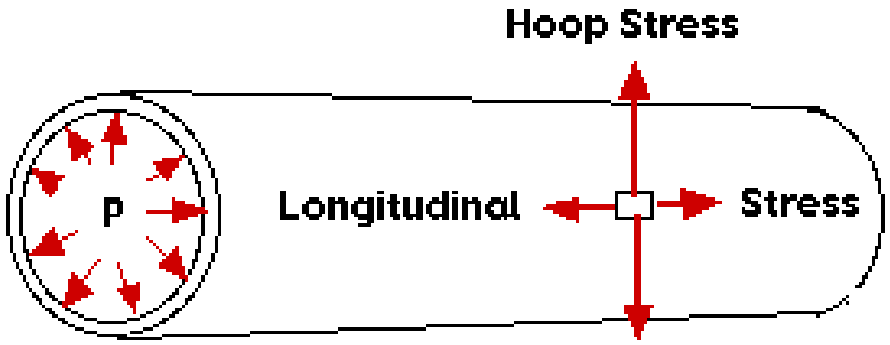

Figure 2.6. 1. Stresses along a cylinder pressure vessel acted by the pressure inside (P) (Pizzo, n.d.).

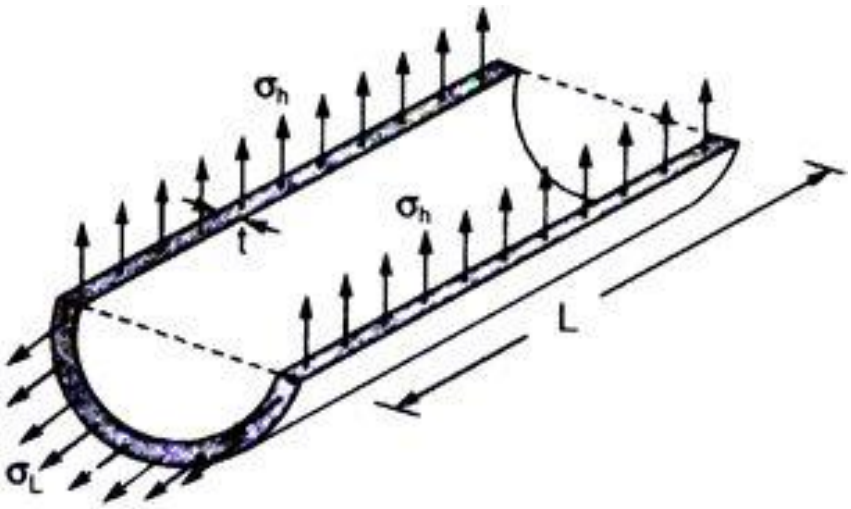

Figure 2.6. 2 Cross section of stresses along a cylinder pressure vessel. σh represents the hoop stress while σL represents the longitudinal stress acting on the wall of the pressure vessel. The thickness (t) and length (L) of the cylinder are also repreted (Patel, 2016).

Chapter 3: Materials and Methods

The outer shell of the cylinder sample was printed out of the thermoplastic, PLA and the interior of the cylinder was filled and compacted with Unimin sand. PLA was chosen because its properties fit the 3D printer's limitations. Table 3.1 shows the PLA's mechanical properties.

Table 3.1. Mechanical properties of PLA (Makeitfrom, 2015).

Elongation	6%
Flexural Modulus	4 GPa
Compressive Strength	18 MPa
Tensile Strength	50 MPa
Shear Modulus	2.4 GPa
Density	1.3 g/cm^3

The soil used for this research was Unimin Silica sand (GRANUSIL 4030); a Cohesionless soil. This type of sand is produced from very high purity industrial quartz sand throughout North America to produce silica sand. This type of soil was used because it is readily available; easy to reproduce results, negligible moisture content, and no clay particles; which eliminates the cohesion acting inside the sample. Unimin Sand has consistently uniform grain shapes and particle size distribution, which allows for great compaction throughout the samples. The following properties were obtained for the soil and can be seen in Table 3.2 and Table 3.3.

Table 3.2. Unimin Sand properties.

Grain Shape	Rounded	Visual
Hardness	7.0 Mohs	Mohs Scale
Moisture Content	<0.1%	ASTM C-566
Specific Gravity	2.65 g/cm^3	ASTM C-128
Bulk Density, aerated	92-95 lb/ft^3	ASTM C-29
Bulk Density, compacted	98-100 lb/ft^3	ASTM C-29

Table 3.3. Grain size distribution table obtained for Unimin 4030 sand.

	Mesh ASTM E-11	4030
	16	---
Typical Mean %	20	---
Retained on	30	0.1
Individual	40	22.5
Sieves	50	54.7
	70	17.4
	100	4.2
	140	0.9
	200	---
	270	---
	PAN	0.2

The sand inside the cylinder sample will act like a pressure vessel when the distributive load (F) from the compressive machine acts on it. The sand inside the cylinder will be distributed outward and thus creating several stresses along the walls of the cylinder as shown in Figure 3.1. As described earlier, the two main stress that will act on it and govern are longitudinal and hoop stress.

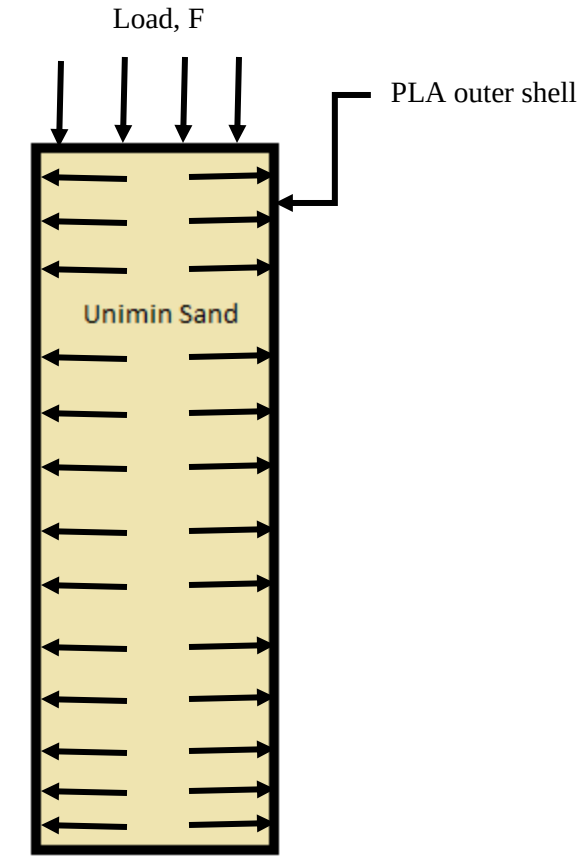

Figure 3.1. This figure represents the axial load, F, distributing the sand inside the cylinder, thus acting like a pressure vessel.

The steps shown in Figure 3.2 were performed to analyze the samples.

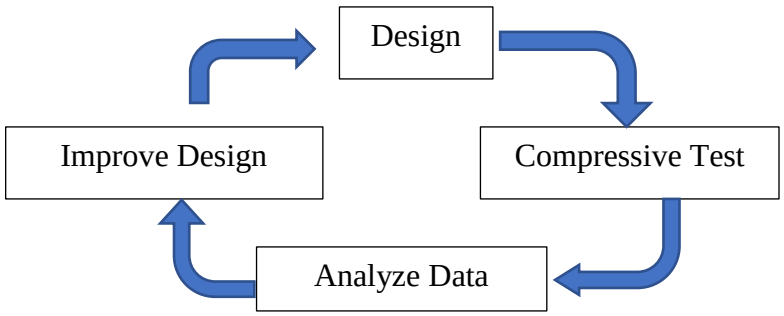

Figure 3.2. Design process.

3.1 Sample Identification

This research included two different designs where the difference between them was the location of how the seam (Z seam) was printed. Each design had the same number of samples that were filled with sand and samples with no sand present. These are identified in Table 3.1.1.

Table 3.1. 1. Design samples' abbreviations.

Design number and Name	Abbreviation
Design 1: Normal Z seam with/without sand	S or NS
Design 2: Randomized Z seam with/without sand	RS or RNS

3.2 First Design

The first design of the composite member was a hollow cylinder with a 2 inch outer diameter and 1.8 inch inner diameter. The thickness of the wall was designed at 0.1 inch. This was designed to analyze for the stresses in a thin walled vessel which states that the ratio between the wall thickness and the radius must not exceed 1/10. The hollow cylinder was designed using SolidWorks. SolidWorks is a solid modeling computer-aided design (CAD) and a computer-aided engineering (CAE) computer program. This program is easy to use, easy to learn, it’s faster, which leads to a more cost effective way. According to an MIT survey in 2006, it provided a better visualization design, better products, faster design iterations, improved communications, design with fewer errors, and creates more aesthetic designs which is why it was used. Figure 3.2.1 shows the height of

the sample while Figure 3.2.2 shows the inner diameter and thickness of the cylinder.

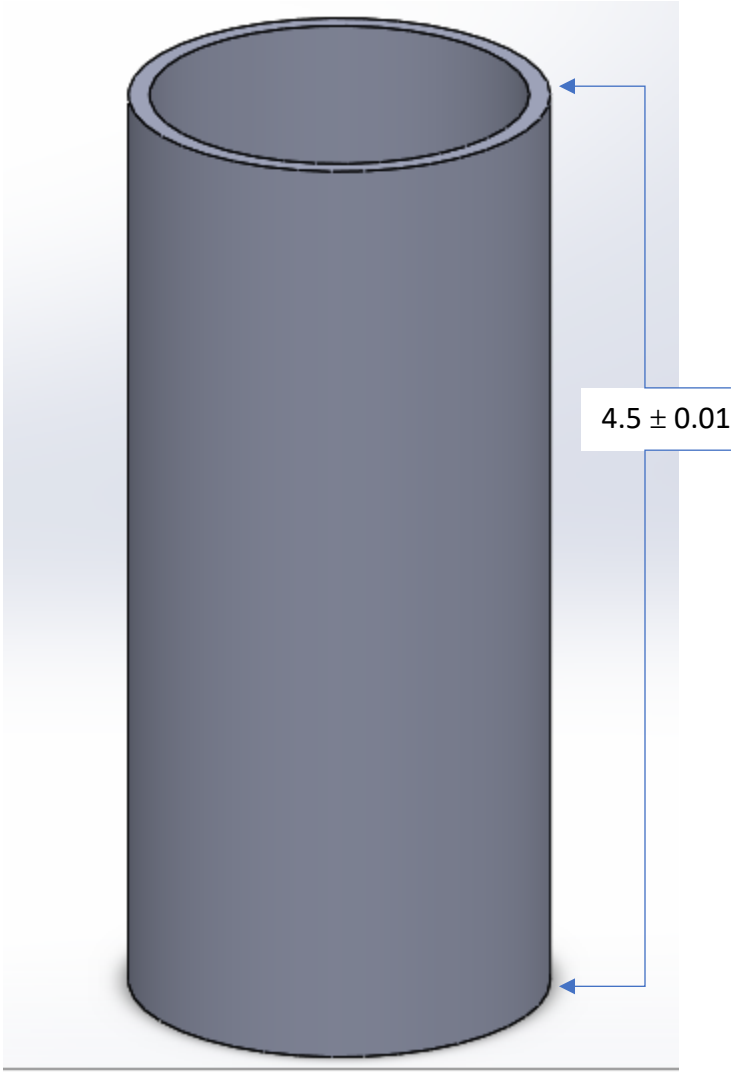

Figure 3.2.1. Dimensions for the cylinder height of 4.5 inches.

There were two end caps that were also designed for the bottom and the top of the cylinder. The caps were designed separately from the cylinder and later checked after printing to ensure a snug fit. The dimensions for the cylinder and caps were measured using SolidWorks as illustrated in Figure 3.2.2 through Figure 3.2.5.

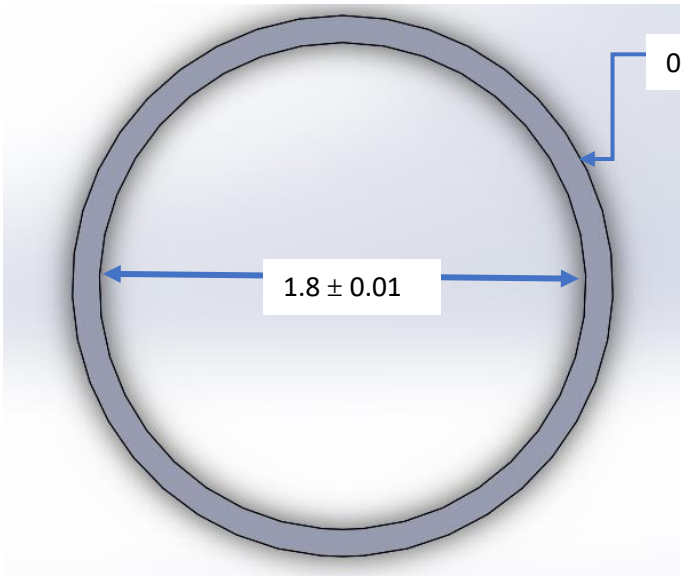

Figure 3.2.2. Dimensions for the cylinder inner diameter of 1.8 inches and thickness of 0.1 inches.

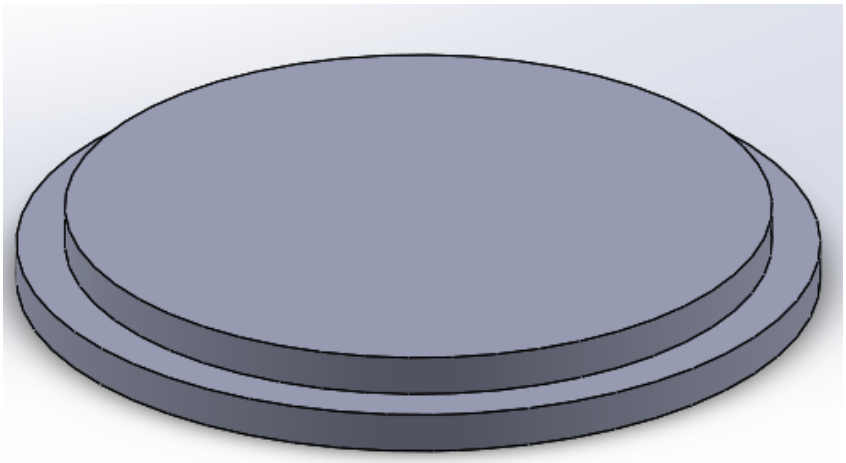

Figure 3.2.3. Drawing of end caps.

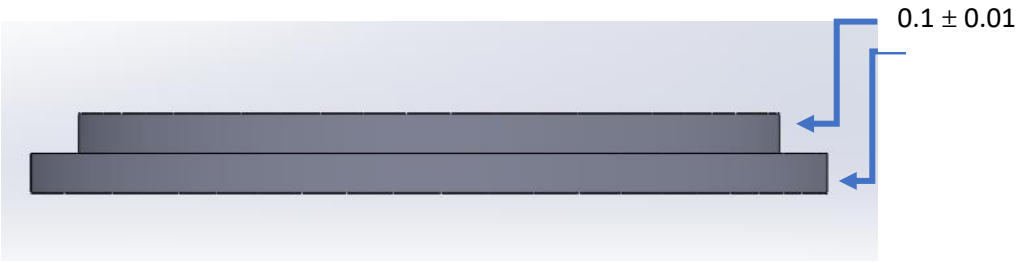

Figure 3.2.4. Dimensions for the cylinder caps with a thickness of 0.1 inches.

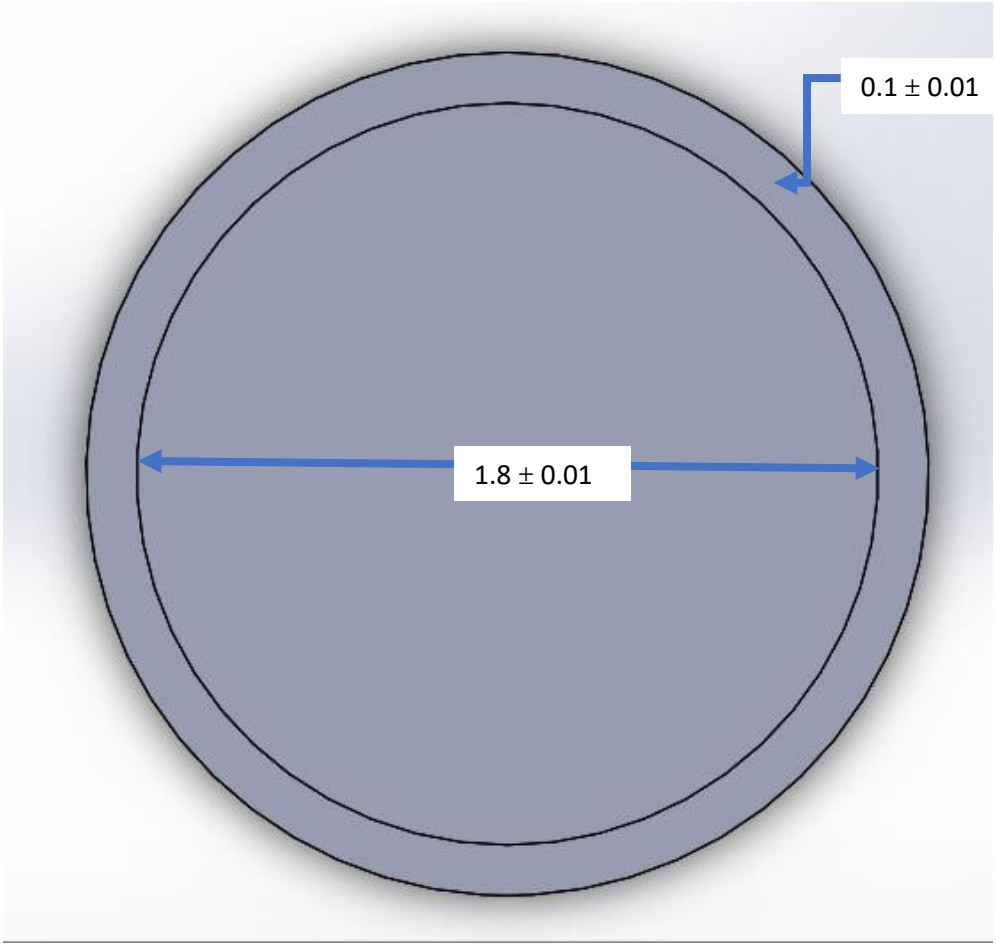

Figure 3.2.5. Dimensions for the cylinder caps with an inner diameter of 1.8 inches and thickness of 0.1 inches.

Then, the cylinder samples and caps were printed using the 3D printer, Flash Forge Creator Pro©, and PLA filament as the printing material. For the printer to print PLA the nozzle temperature had to be at least 200ºC and the platform had to be 110 ºC. A schematic of the printer's plate and nozzle locations are shown in Figure 3.2.6. Room temperature where the 3D printer is printing must be kept at a constant 23 ºC ± 2ºC for the printer to print properly.

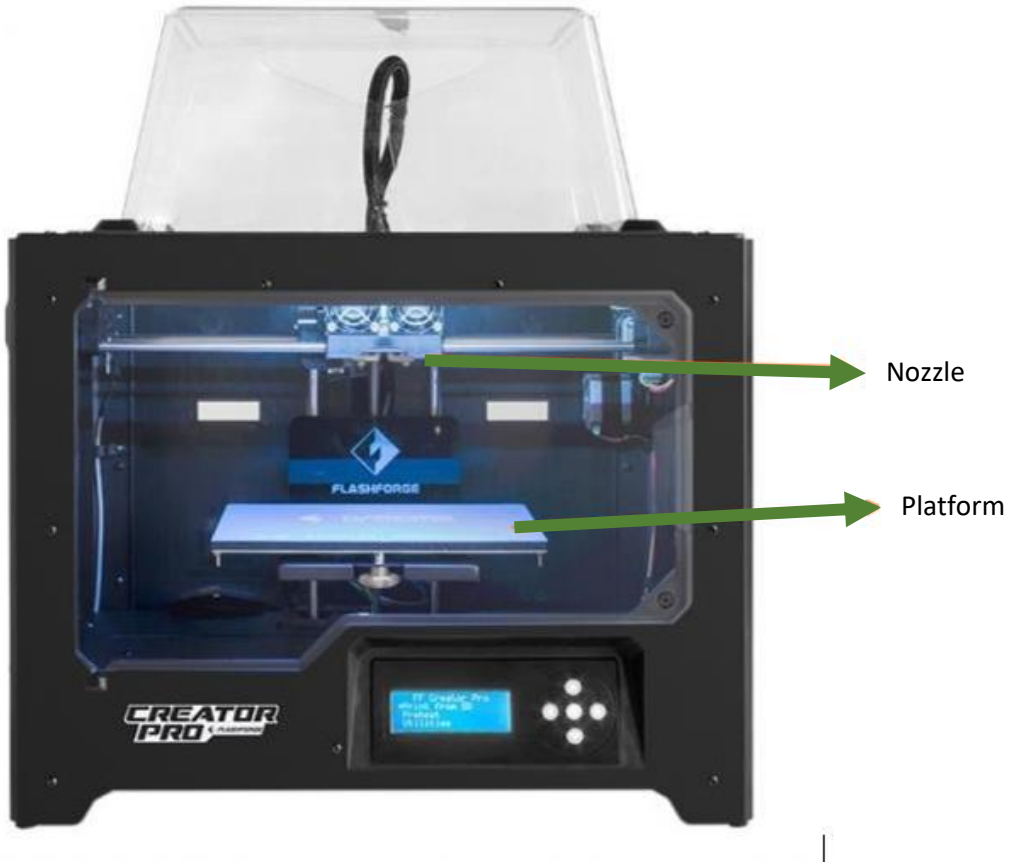

Figure 3.2.6. The location of the Nozzle and Platform in the creator pro 3D printer.

The following parameters were used for the first design of the cylinder. The nozzle temperature was set at 200°C while the bed temperature was set at 120°C for the print. The in-fill was set to 15% fill for the cylinder walls and caps.

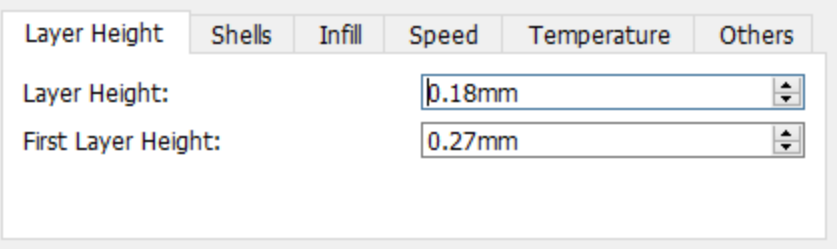

Figure 3.2.7. The layer height parameters set on Flashprint.

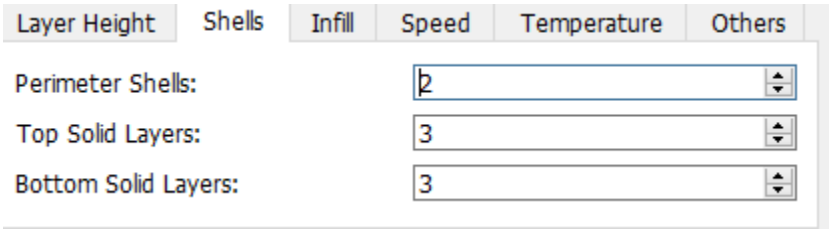

Figure 3.2.8. The shell parameters set on Flashprint.

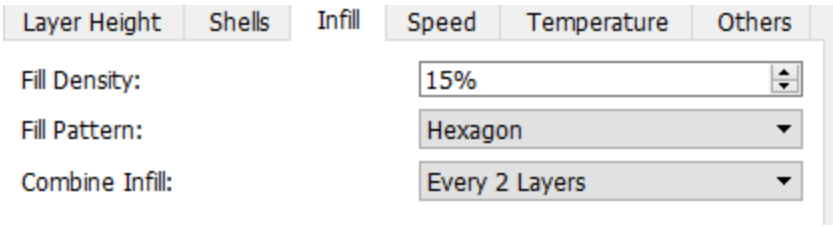

Figure 3.2.9. The infill parameters set on Flashprint.

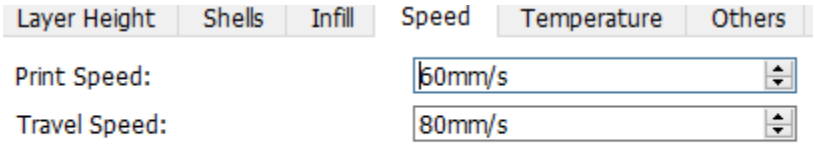

Figure 3.2.10. The speed parameters set on Flashprint.

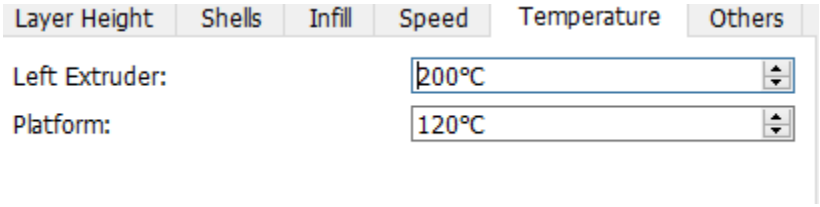

Figure 3.2.11. The temperature parameters set on Flashprint.

3.3Compacting.

The samples were kept in a dry cabinet where the humidity and temperature stayed constant. They were then compacted with the Unimin sand. There is not a standard for compacting these particular cylinder samples, so a method was devised. The cylinder was capped on one end and the sand was filled through the top of the cylinder to a third of the way. A thin metal rod wad used to rod and compact the sand inside. Rodding consisted of 15 times in a circular method. The sides of the cylinder were tapped with a small like hammer a total of 15 times per layer. This process was repeated until all of the sand that was measured was inside the cylinder. The sand inside the sample was designed to have a relative compaction of 50%-60%. The following equations were used to determine the amount of soil needed to fill the cylinders with. Values for void ratio for a fine sand were obtained in Table 3.3.1.

Table 3.3.1. Typical values of void ratio (e) provided from Das.

Soil Type	Void Ratio e	
	Max	**Min**
Fine Sand	0.85	0.40

$$D_r = \frac{e_{max} - e}{e_{max} - e_{min}} \times 100$$ Equation 3.1

Where;

D_r = relative compaction (%)

e_{max} = the maximum void ratio

e_{min} = the minimum void ratio

e = the desired void ratio

$$e = \frac{V_V}{V_S}$$ Equation 3.2

Where;

V_v = the volume of voids

V_s = the volume of solids

$$V_V = V_T - V_S$$ Equation 3.3

Where;

V_T = the total volume

$$V_S = \frac{M_S}{G_S \times \rho_W}$$ Equation 3.4

Where;

M_s = the mass of solids

G_s = the specific gravity of Unimin sand

ρ_w = the density of water

Using these equations the total amount of soil needed for each soil sample was determined. Tables 3.3.2 and 3.3.3 show the different weights calculated for the each of the cylinder samples.

Table 3.3.2. The different weights for the first design with sand filled cylinders.

Z seam	Cylinder (g)	Caps (g)	Sand (g)	Total (g)
1	69.64	3.50	293.36	366.50
2	70.17	3.50	292.99	366.66
4	72.97	3.50	299.55	376.02
5	69.78	3.50	301.88	375.16

Table 3.3.3. The different weights for the second design with sand filled cylinders with randomized location of the Z seam.

Random	Cylinder (g)	Caps (g)	Sand (g)	Total (g)
1	61.04	3.50	298.08	362.62
2	62.26	3.50	302.56	368.32
3	63.91	3.50	292.33	359.74
4	62.06	3.50	298.42	363.98

3.4 Compressive Testing.

Compressive strength was defined as the resistance of a member to breaking under compression. The apparatus used to perform the compressive test was a MTS 370 Landmark which can provide loads up to 100 kN (22,000 lbs), as seen in Figure 3.4.1. The sample was placed in the center of the apparatus, upright with the caps on the top and bottom, and tested by applying a distributive load at the top of the cylinder. As the sample is being tested the data from the MTS 370 Landmark was recording simultaneously, providing force and displacement data.

Figure 3.4.1. Compressive test apparatus setup.

3.5 Analyzing the Data

To perform the compressive analysis and obtain the properties of the samples the force-displacement data obtained was plotted and used to calculate the different stress data using Excel.

1) Pressure acting on the cylinder sample was obtained using Equation 3.5

$$p = \frac{F}{A}$$ Equation 3.5

Where;

p = pressure

F = the applied load

A = the cross sectional area of the sample

2) The Longitudinal Stress was calculated using Equation 3.6

$$\sigma_l = \frac{p \times d_i}{2 \times t} \quad \text{Equation 3.6}$$

Where;

σ_l = is the longitudinal stress [Force/Area]

di = is the inner diameter [Length]

t = is the thickness of the wall [Length]

3) The Hoop Stress was calculated using Equation 3.7

$$\sigma_c = \frac{p \times d_i}{t} \quad \text{Equation 3.7}$$

Where;

σ_c = is the circumferential stress [Force/Area]

4) Stress-strain graphs were then obtained using excel, having the stress on the y-axis and the strain on the x-axis.

5) Mechanical properties were obtained from the stress-strain graphs.

6) Comparing all the similar samples together and estimating the standard deviation using Equation 3.8

$$s = \sqrt{\frac{(\sum x^2 - nX^2)}{n-1}} \quad \text{Equation 3.8}$$

Where;

S = the standard deviation

x = value of a single observation

X = mean value of the set of observation

n = number of observations

3.6 Quality Control

For quality control four samples were printed for every design in this experiment. Since the printer is programmed for extreme accuracy, the samples dimensions matched within 0.01 in. The dimensions were checked after printing using a digital caliper to ensure the accuracy of the print. When testing samples S-3 and NS-3, the compressive machine broke and the test was not able to continue. Once a test started it could not be stopped and then started back up. This is the reason why samples S-3 and NS-3 are excluded from the data set. The samples were not renumbered to tell them apart from each other.

Chapter 4: Research Results and Discussion

To determine the different stresses acting on the structural member, the research was dived into the following continuous cycle: First Design, Second Design, Compare & Contrast, and Failure Mechanisms.

4.1 First Design

The first design was to analyze the cylinder with sand to determine the different types of pressures acting inside the sample. Figure 4.1.1 shows how a typical force-displacement graph should look like for the samples with sand. Some key points to note in the figure are points A and B. Point A is where the member reaches its maximum axial capacity before the sample starts to fail. Point B is when complete failure occurs and the sample fails catastrophically.

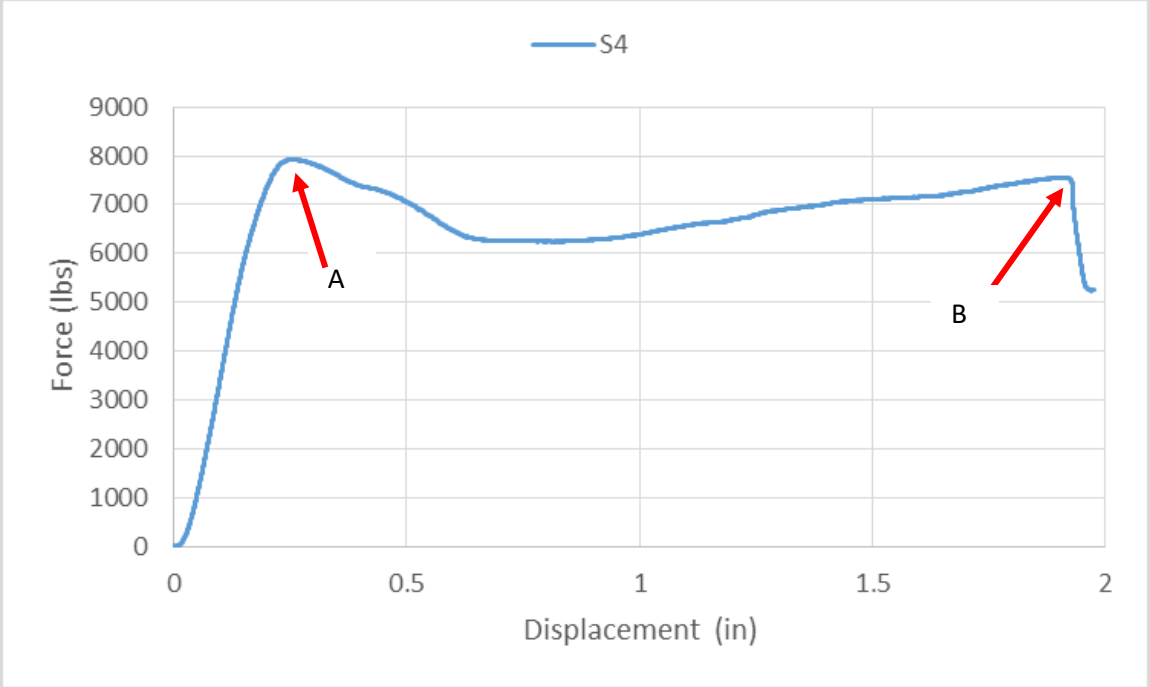

Figure 4.1.1. Typical force-displacement data for sand filled samples; sample S-4.

Sample S-1 was used to get familiar with the apparatus and thus the results don't represent the whole data, but are included as a comparison among the samples. Figure 4.1.2 shows sample S-1 and a critical point; point A. Point A occurred in this set of sample only and is where the sample starts to yield and fail before starting to regain strength again.

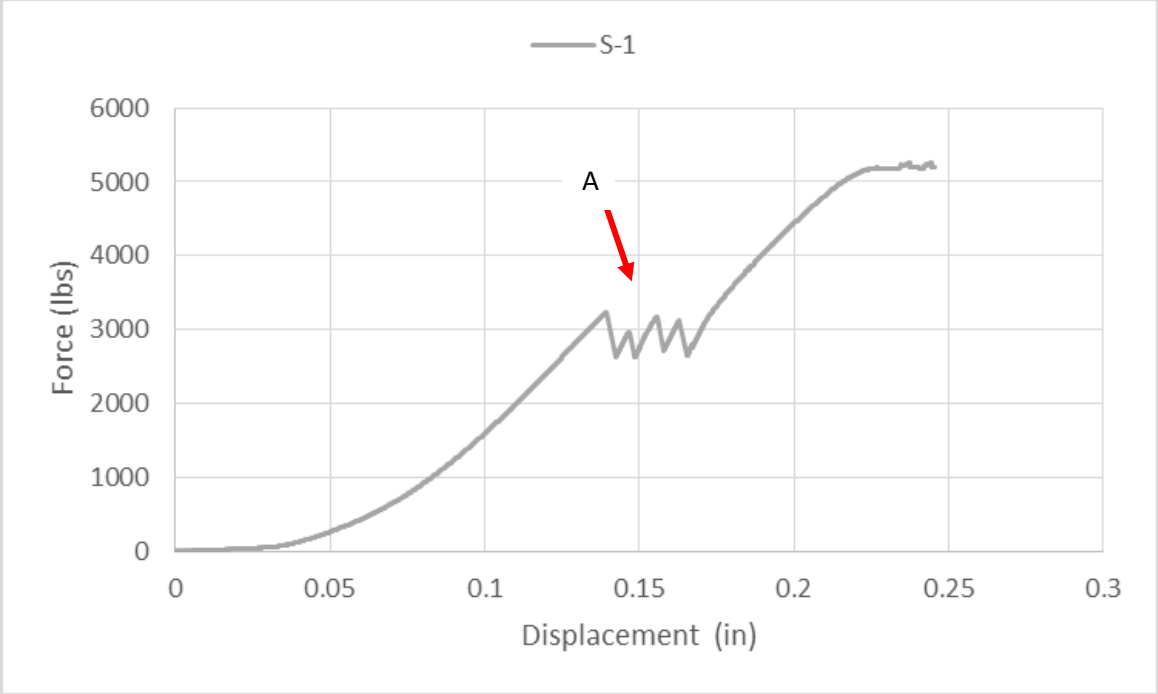

Figure 4.1.2. Sample S-1 with critical point; Point A.

The four samples were tested and the results were compared. Figure 4.1.2 is a force-displacement graph that illustrates the maximum forces for each of the different samples filled with sand before failure.

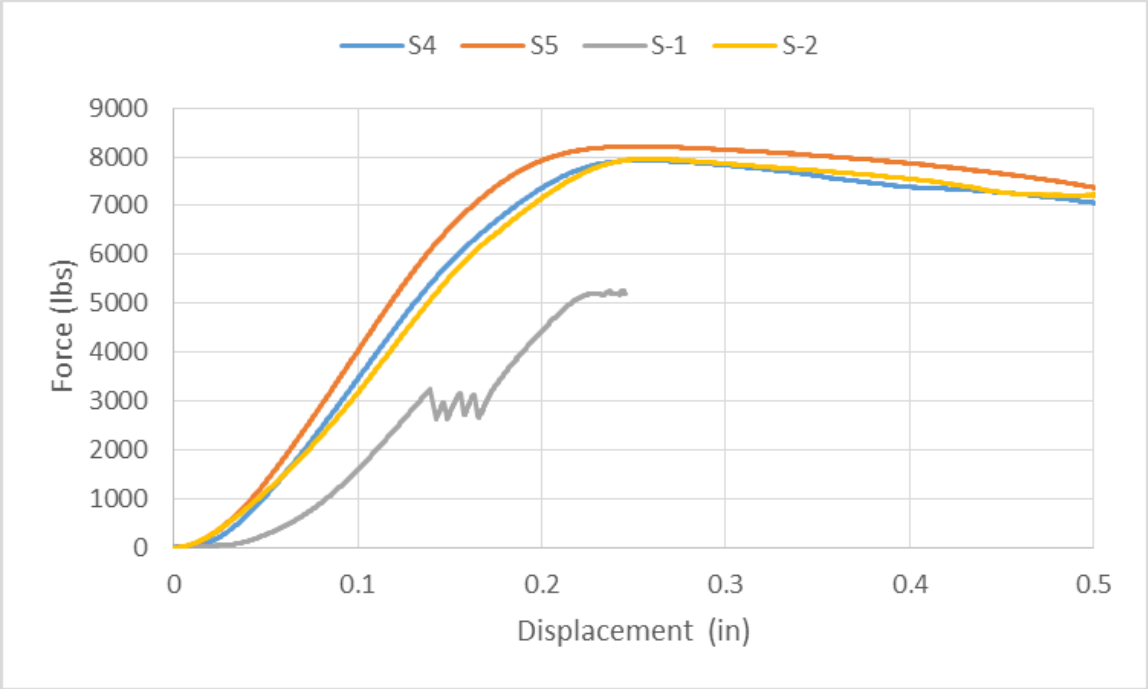

Figure 4.1.3. Force-displacement data for sand filled samples displaying the maximum force.

The maximum values for each sample were taken from Figure 4.1.3 and can be seen in Table 4.1.1. An average was taken between samples S-2, S-4, and S-5. The reason that S-1 was not included in the average was because the value was outside the standard deviation when compared to the others due to some source of unknown error in the data, but was left in the data for comparison.

Table 4.1.1. Maximum force each of the sand filled cylinders held. (n=3)

Z seam	S-1*	S-2	S-4	S-5	Average
Max force (lbs)	5,264	7,963	7,931	8,216	8,037 ± 156

A second set of samples were tested to determine how the cylinders would behave without the soil inside. Figure 4.1.4 shows a force-displacement graph that illustrates the maximum forces for each of the different samples without any sand present.

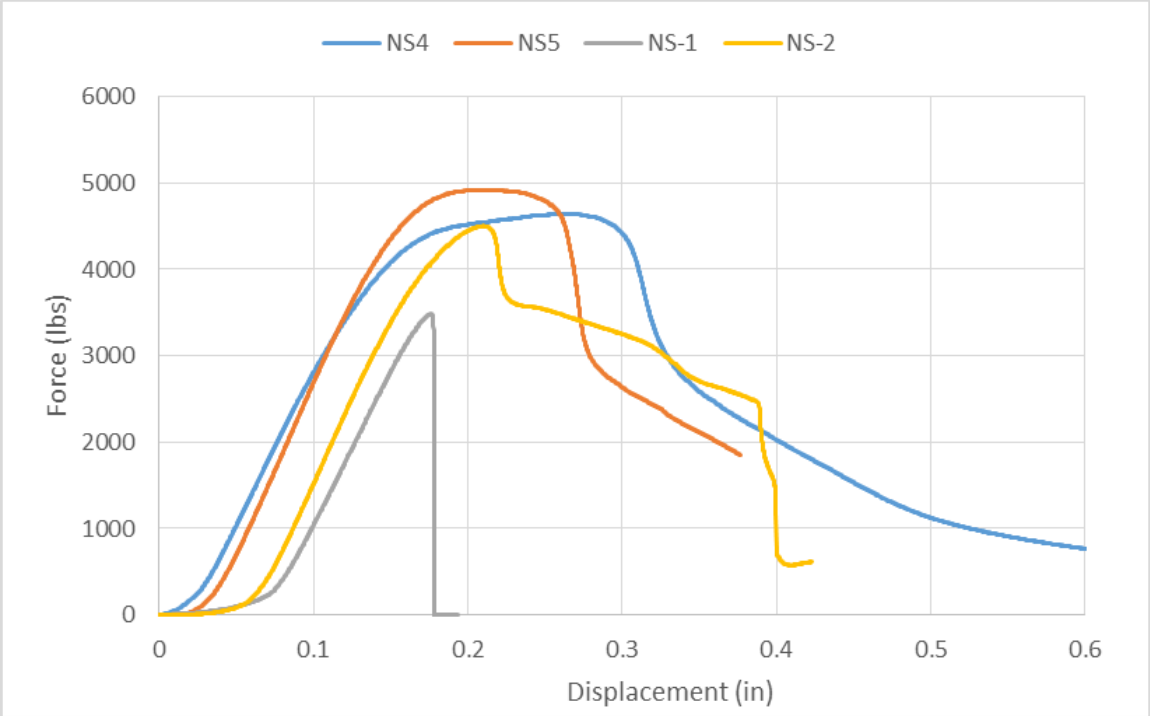

Figure 4.1.4. Force-displacement data for hollow samples.

The maximum values for each sample were taken from Figure 4.1.4 and can be seen in Table 4.1.2. An average was taken between samples NS-2, NS-4, and NS-5. The reason that NS-1 was not included in the average was because the value was outside the standard deviation when compared to the others due to some source of unknown error in the data, but was left in the data for comparison.

Table 4.1.2. Maximum force for each of the hollow cylinders. (n=3)

Z seam	NS-1*	NS-2	NS-4	NS-5	Average
Max force (lbs)	3,483	4,503	4,641	4,921	4,688 ± 213

From the maximum force data presented in Table 4.1.2, Pressure, Longitudinal stress, and Hoop stress were calculated and tabulated in Table 4.1.3 for the samples with sand.

The average and standard deviation between them were calculated. The stress acting on the hollow cylinder walls was also calculated and tabulated in Table 4.1.4.

Table 4.1.3. Tabulated Stresses for the cylinders with sand. (n=3)

Z seam	S-1*	S-2	S-4	S-5	Average
Pressure (psi)	2,068	3,129	3,117	3,229	3,158 ± 61
Long stress (psi)	18,616	28,163	28,050	29,058	28,424 ± 552
Hoop stress (psi)	37,233	56,327	56,101	58,115	**56,848 ± 1104**

Table 4.1.4. Axial Compression Stress acting on hollow cylinder. (n=3)

Z seam	NS-1*	NS-2	NS-4	NS-5	Average
Stress (psi)	5,835	7,544	7,775	8,244	**7,854 ± 356**

It was noted that the samples with the sand resisted a maximum force of 8,038 lbs, which is a 170% increase when compared to the hollow samples of 4,688 lbs. When comparing the different stresses, the Hoop stress is among the highest stress calculated between all of the samples at 56,848 psi and is the most critical. The stresses in the sand filled samples were also much higher when compared to the hollow samples. Every sample with filled sand developed interlayer adhesion failure along the seam of where the print started and stopped, this this seam is referred to as the Z seam and is shown in Figure 4.1.5.

Figure 4.1.5. Location of the Z seam with respect to the sample.

4.2 Second Design

A second design to reduce the interlayer adhesion failure at the Z seam was designed. After some research, it was determined that the seam of the samples can be randomized when printing. This was a setting in the printing parameters of the Flashprint software. The cylinders where printed with the same parameters and had the exact same dimensions except with randomized start stop points for each layer of print. The same

parameters as the first design for printing and for compacting were used to ensure quality results. To access the randomized Z seam print mode the Flashprint software must be switched to “Expert Mode” from “Basic Mode” as seen in Figure 4.2.1. The Preference window can be found under the File tab in the upper left hand corner.

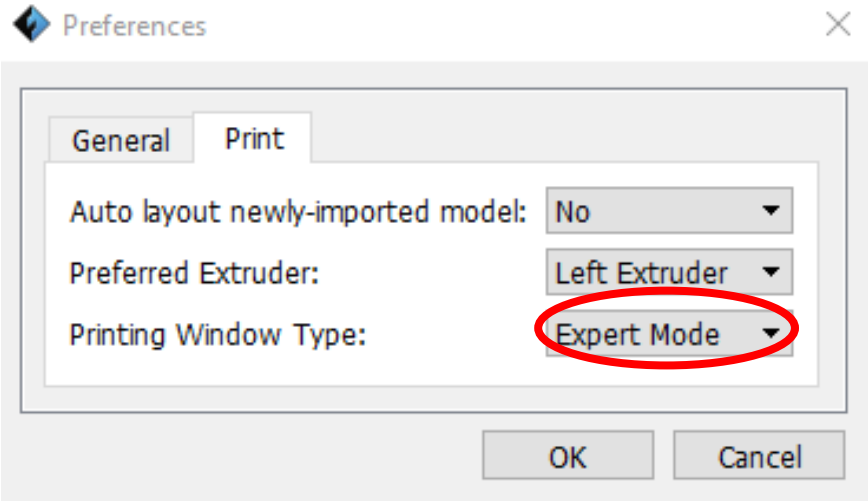

Figure 4.2.1. Print preference mode for Flashprint software.

Once in expert mode, load a file and continue to the print section window. Under the perimeter tab, make sure that the more for start points is set to “use random start points” as illustrated in Figure 4.2.2. This adjusts the location of where the extruder nozzle starts each new layer of the print. Setting the layer perimeter to print randomly allows for the Z seam to not be visible which can be seen in a printed sample in Figure 4.2.3.

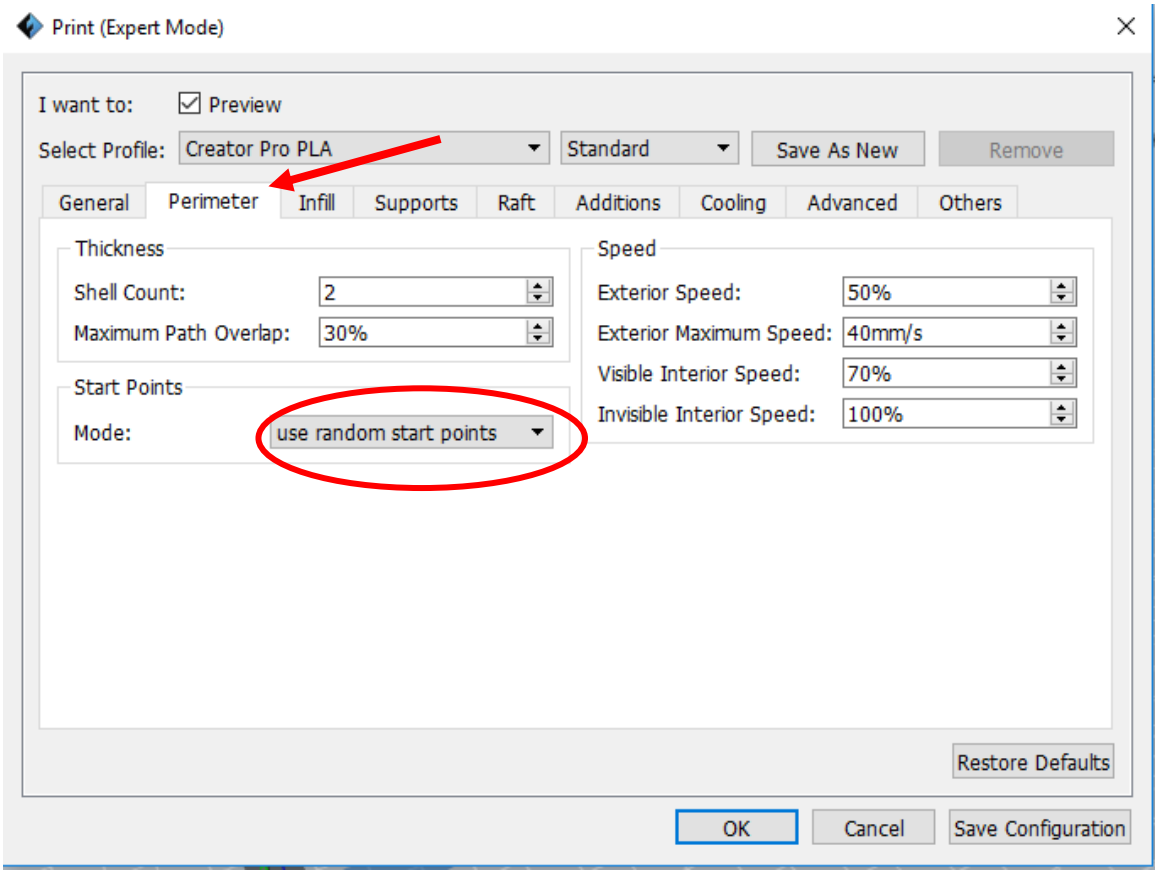

Figure 4.2.2. “Start Points” mode for randomized Z seam printing.

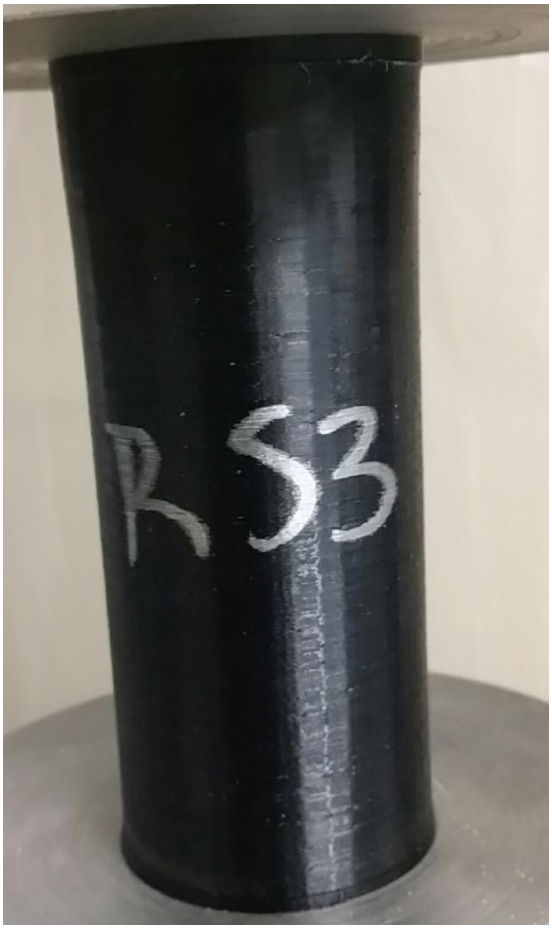

Figure 4.2.3. Sample RS3 with the randomized Z seam print.

Four different samples were printed of sand filled cylinders and hollow cylinders each for comparison. The second design was aimed to analyze the cylinder with sand with randomized Z seam and determine the different types of stresses acting inside the sample. Figure 4.2.3 is a force-displacement graph that illustrates sample RS1 carried out to its maximum failure and used as a comparison, noting the maximum force capacity.

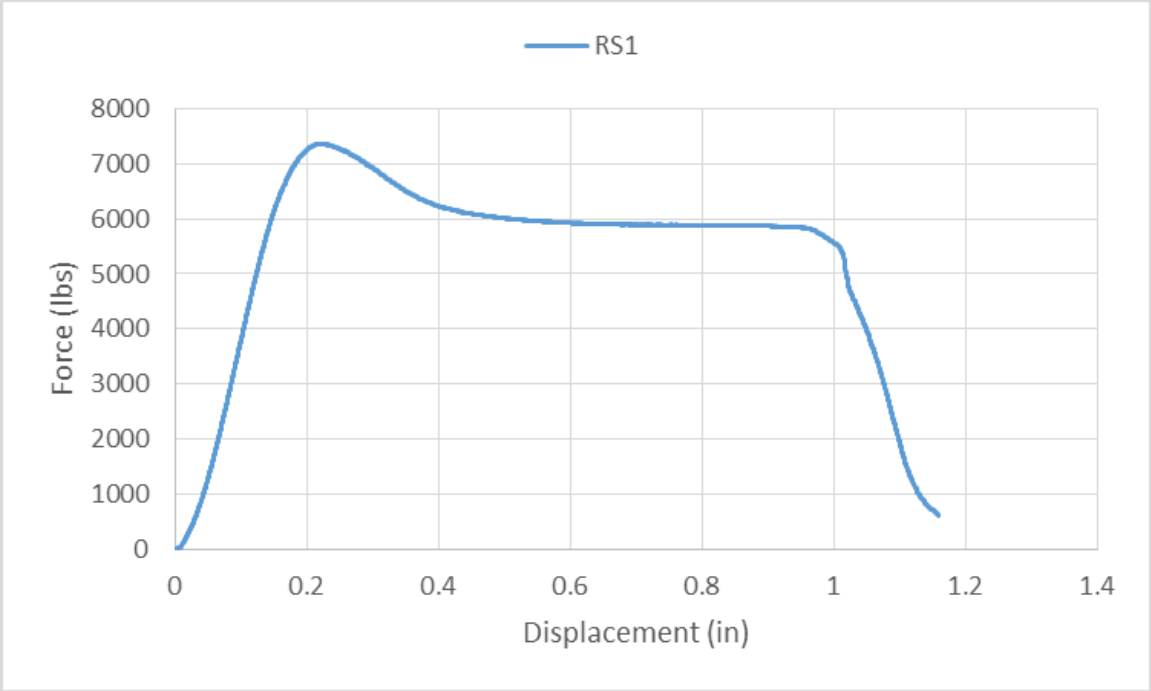

Figure 4.2.4. Typical force-displacement data for randomized Z seam sample.

After testing all four samples, the force-displacement was graphed and the data can be seen in Figure 4.3.5 below. It is noted that not all the samples were taken to maximum failure, for efficiency purposes and were stopped at 20% of their maximum force.

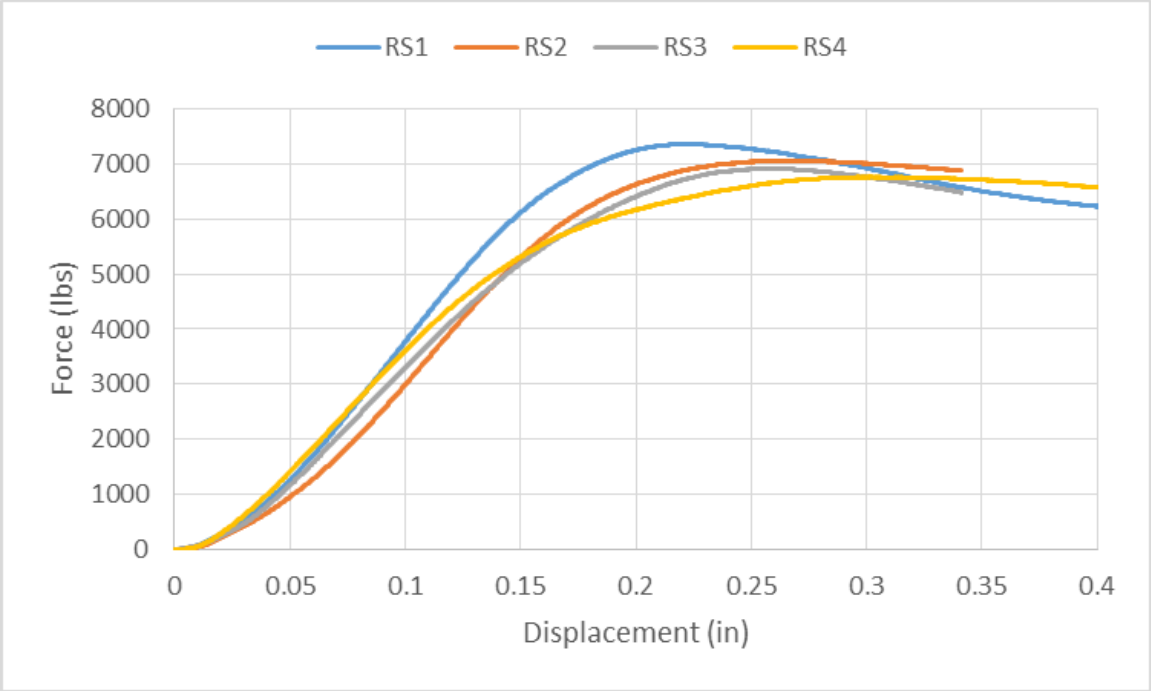

Figure 4.2.5. Force-displacement data for randomized Z seam, sand filled samples.

The maximum values for each sample were determined from Figure 4.2.5 and tabulated in Table 4.2.1.

Table 4.2.1. Maximum force for each of the randomized Z seam, sand filled cylinders. (n=4)

Random	RS-1	RS-2	RS-3	RS-4	Average
Max force (lbs)	7,363	7,057	6,913	6,765	7,025 ± 255

A second set of samples were tested to determine how the cylinders would behave without the soil present. Figure 4.2.6 shows the force-displacement data that illustrates the maximum forces for each of the different samples without any sand present with a randomized Z seam.

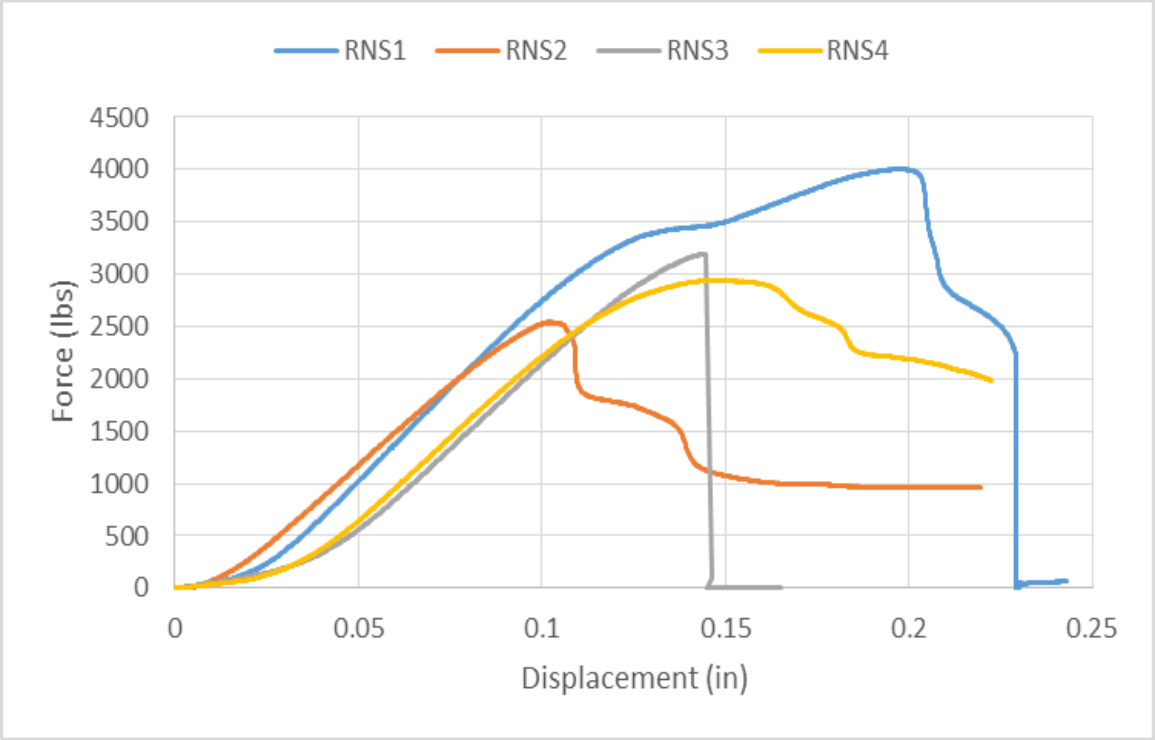

Figure 4.2.6. Force-displacement data for randomized Z seam, hollow samples.

The maximum values for each sample were determined from Figure 4.2.6 and tabulated in Table 4.2.2.

Table 4.2.2. Maximum force for each of the randomized Z seam, hollow cylinders. (n=4)

Random	RNS-1	RNS-2	RNS-3	RNS-4	Average
Max force (lbs)	4,002	2,540	3,195	2,940	3,169 ± 617

From the maximum force data obtained in Table 4.2.2, the Pressure, Longitudinal stress, and Hoop stress were calculated and tabulated in Table 4.2.3 for the samples with sand with randomized Z seam. The stress acting on the hollow cylinder walls was also calculated and tabulated in Table 4.2.4.

Table 4.2.3. Tabulated Stresses for the cylinders with sand with randomized Z seam. (n=4)

Random	RS-1	RS-2	RS-3	RS-4	Average
Pressure (psi)	2,893	2,773	2,717	2,658	2,760 ± 100
Long stress (psi)	26,040	24,960	24,451	23,925	24,844 ± 902
hoop stress (psi)	52,080	49,921	48,903	47,850	**49,688 ± 1805**

Table 4.2.4. Axial Compression Stress acting on hollow cylinder. (n=4)

Random	RNS-1	RNS-2	RNS-3	RNS-4	Average
Stress (psi)	6,705	4,256	5,353	4,925	**5,310 ± 1034**

It was noted that the samples with the sand resisted a maximum force of 7,025 lbs, which is a 220% increase when compared to the hollow samples of 3,169 lbs. When comparing

the different stresses, the Hoop stress is among the highest stress calculated between all of the samples at 49,688 psi and is the most critical. The stresses in the sand filled samples were also much higher when compared to the hollow samples.

4.3 Compare & Contrast

After ensuring quality control throughout the samples, the different properties were compared between all of the samples from design 1 and design 2. Figure 4.3.1 illustrates the comparison between the different maximum forces for each set of samples.

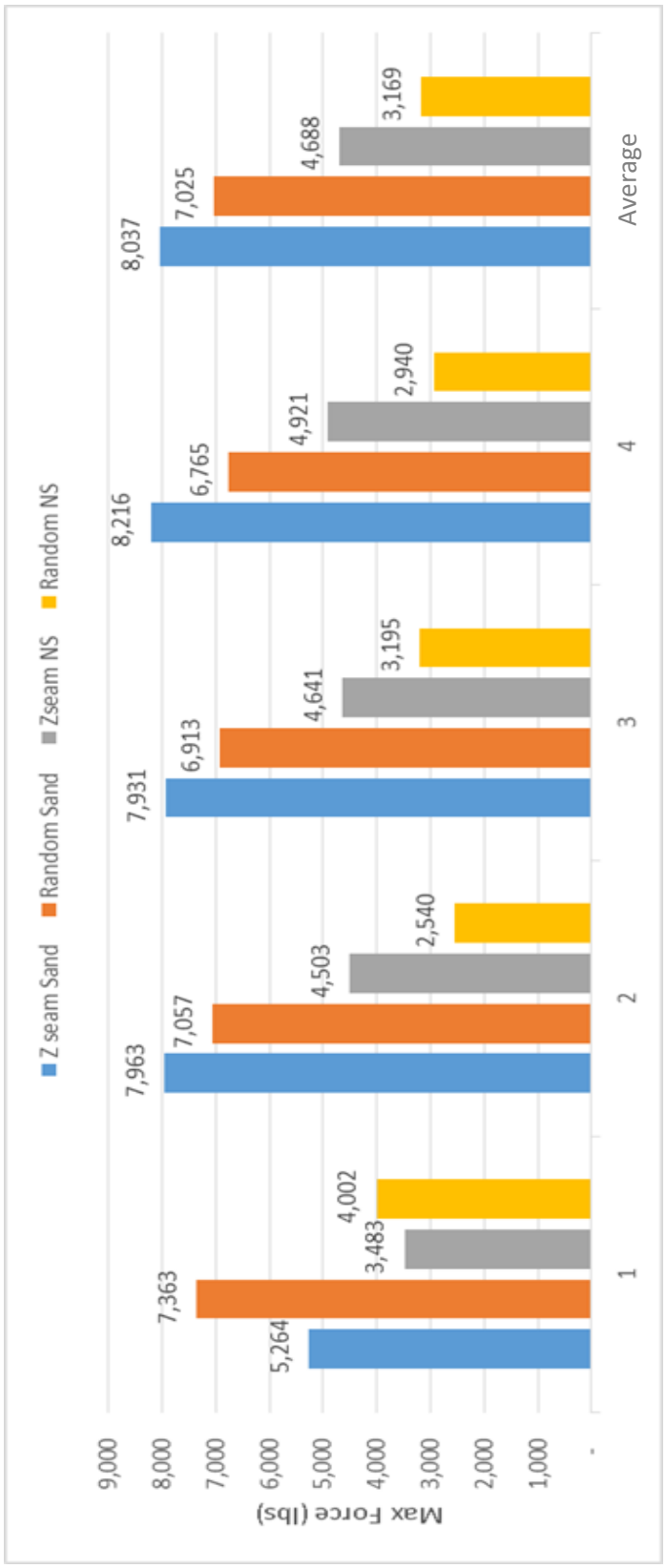

Figure 4.3.1. Comparison of the maximum forces between all the samples.

Figure 4.3.1 illustrates how much the difference the presence of sand inside the cylinder samples helped maximize the force resistance capacity. Comparing the differences between design 1 and design 2, the first design with sand, the maximum force was the largest in all of the samples followed by the randomized Z seam, sand filled samples then the hollow cylinder from design 1, and finally the last was the hollow cylinder with the randomized Z seam. Similar trends followed the average for all the samples. After determining the maximum forces, a comparison of the longitudinal and hoop stresses were made between design 1 and design 2 and can be seen in Figure 4.1.6 and Figure 4.1.7.

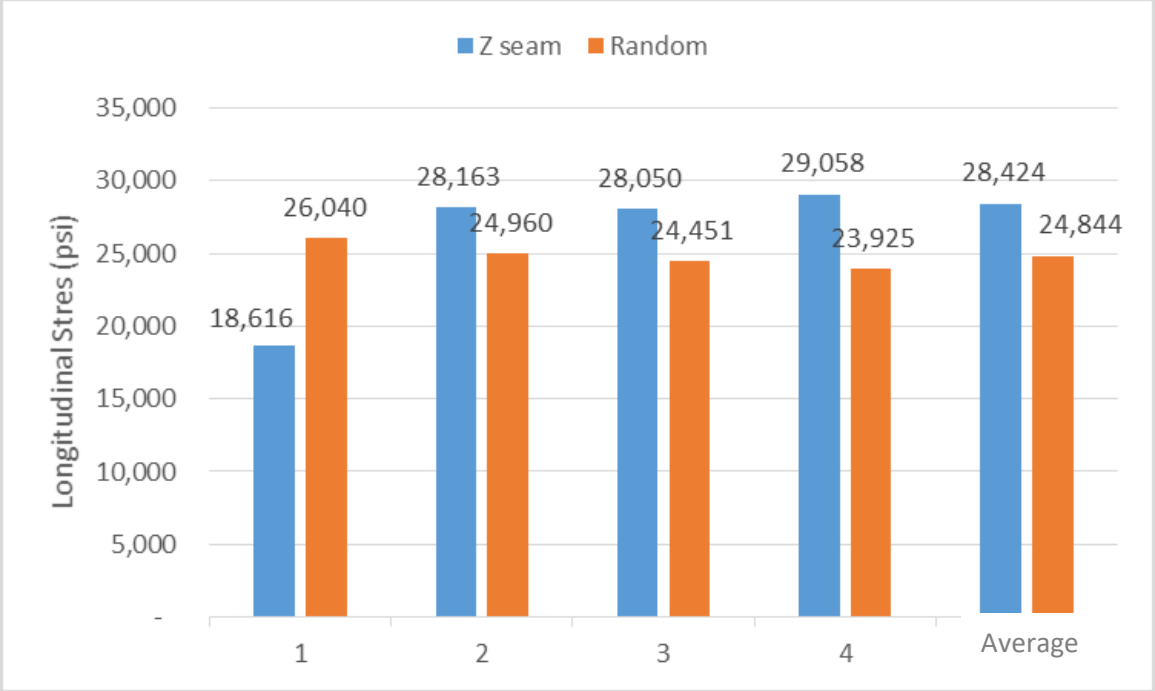

Figure 4.3.2. Comparison of the longitudinal stresses between the Z seam present and the random Z seam.

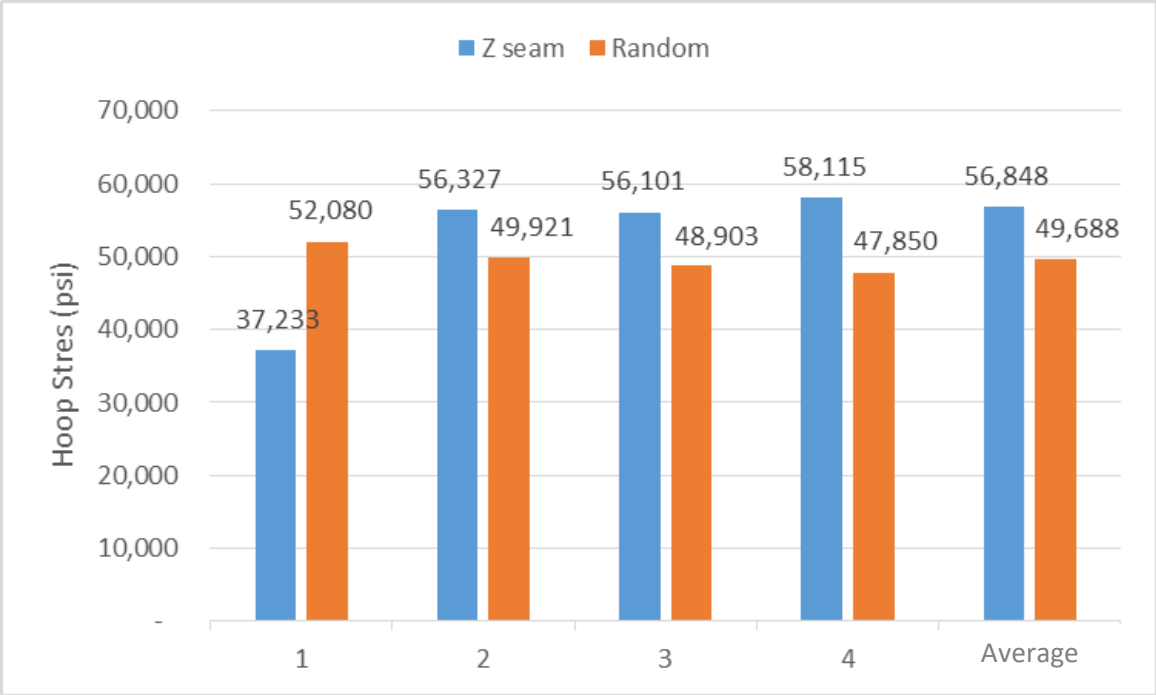

Figure 4.3.3. Comparison of the hoop stresses between the Z seam present and the random Z seam.

It can be observed that the Hoop stresses between the two designs are twice as much as the Longitudinal stresses which leads to suggest that the hoop stress governs and is the most critical among the different stresses acting on the samples. Both the hoop stress and longitudinal stress for the design 1 samples are 15% more than the second design with the randomized Z seam. Hoop stress and ultimate tensile stress of PLA can be compared as seen in Table 4.3.4. The hoop stress from design 1 is 840% more than the ultimate tensile stress of PLA, while the hoop stress from design 2 is 730% more.

Table 4.3.4. Comparison of Hoop Stress and Ultimate Tensile Stress.

	Hoop Stress (psi)	**Ultimate Tensile Stress (psi)**
Design 1	56,848	-
Design 2	49,688	-
PLA	-	6,783

4.4 Failure Mechanisms

A column can fail in one of two ways, either by crushing or by buckling, as explained earlier. The failure caused by the samples were more of a crushing failure than a buckling failure. Compression failure is the material itself crushing or yielding against itself. The applied forces and stresses in the sample are higher than the allowable thus resulting in a crushing failure. Figure 4.4.1 shows the typical failure gathered from design 1 hollow samples. Figure 4.4.2 shows the comparison of the typical failure gathered from design 2 hollow samples.

Figure 4.4.1. Failure of design 1 hollow samples.

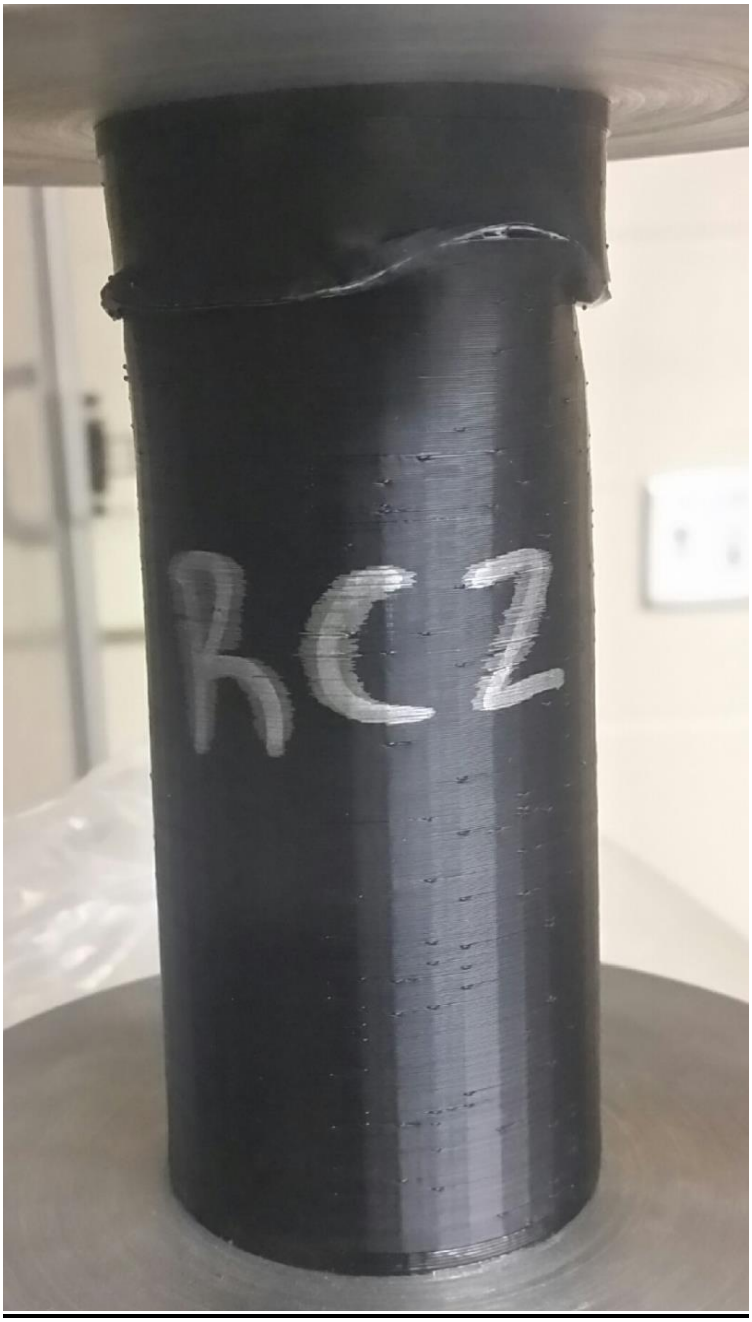

Figure 4.4.2. Failure of design 2 hollow samples.

When the cylinder was hollow, the samples seemed to fail in a slow crushing mode. The sample kept crushing over on itself. Figure 4.4.3 shows the comparison in the data between the two hollow samples with no sand. Once the sample reaches its maximum force capacity, the sample tents to fail in a similar method.

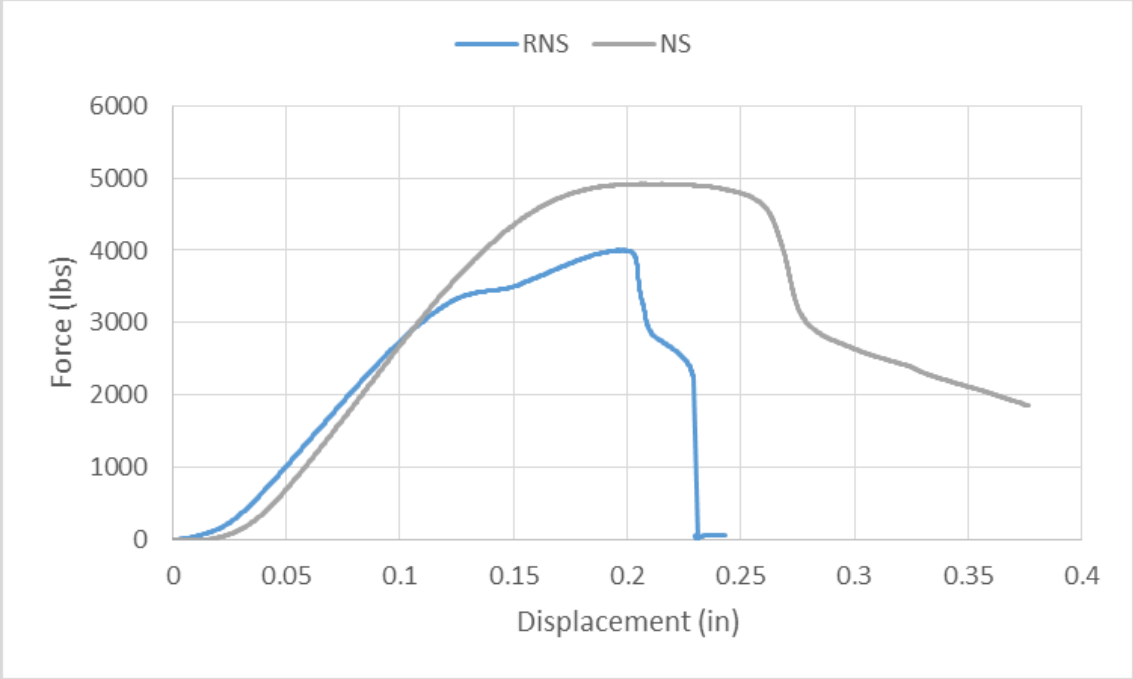

Figure 4.4.3. Failure of design 1 and design 2 hollow samples.

A comparison between the failure modes between the two designs with sand filled cylinders was done. Figure 4.4.4 shows the typical failure gathered from design 2 sand filled samples. Figure 4.4.2 shows the comparison of the typical failure gathered from design 1 sand filled samples.

Figure 4.4.4. Failure of design 2 sand filled samples.

Figure 4.4.5. Failure of design 1 sand filled samples.

When the cylinder was sand present, the samples seemed to fail in a slow crushing mode while the sand bulged out. The sample kept crushing over on itself while expanding the sand further and further out. Figure 4.4.6 shows the comparison in the data between the two sand filled samples.

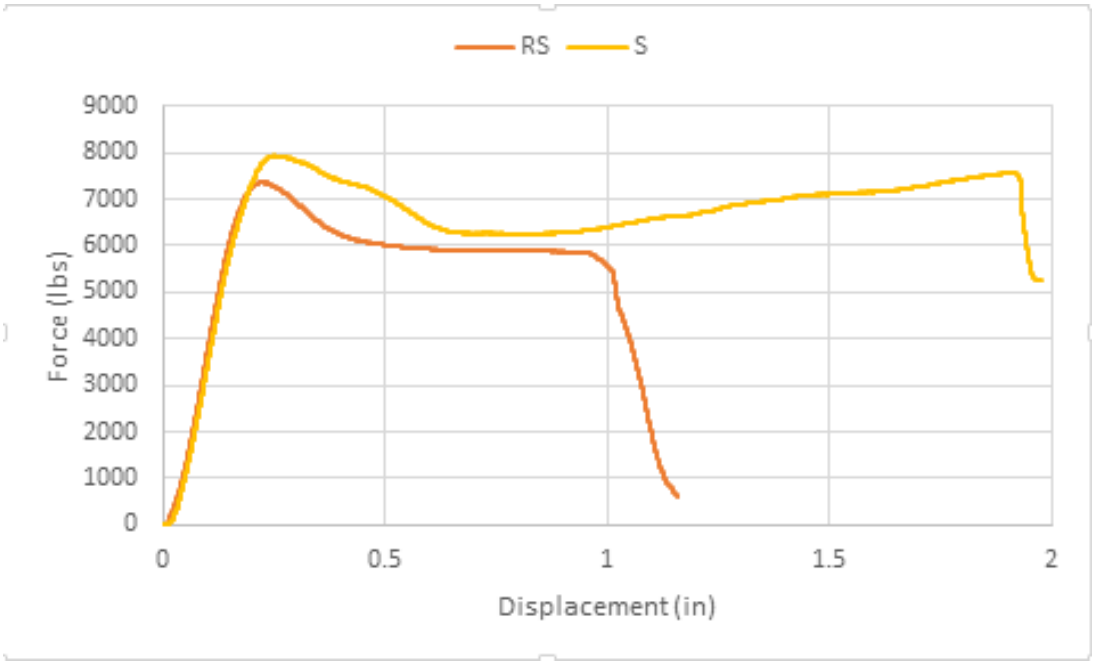

Figure 4.4.6. Failure of design 1 and design 2 sand filled samples.

Once the sample reaches its maximum force capacity, the samples tent to fail in a similar crushing method as the hollow samples. With the addition of the sand, the samples tend to be more ductile, meaning they are able to stretch out more with a constant force being applied. The sand inside the samples helps the cylinders retain at least 75% of the maximum force after beginning to fail. Something interesting when comparing design 1 and design 2 of sand filled samples is that the data for design 1 displaced almost twice as much as the data for design 2.

Conclusion

Utilizing plastics as structural members and locally available soil hits two birds with one stone, since it is affordable and it reduces the plastic waste in the environment. In this research composite beams made of plastic and fine Cohensionless soil were designed, tested, and analyzed to see if it would be sufficient and safe as a structural member. Columns are control by their axial capacity as they transfer the loads from members above, to the existing ground. To perform a compressive testing and analysis of the structural column members, ASTM D695 was followed. In this research, two designs were developed and tested where the newer design was improved from the previous. Design improvements were developed due to undesired failure modes in the interlayer adhesion failure between the Z seam. After testing and comparing the properties of the cylindrical samples, it was concluded that the samples with sand have a higher axial capacity that the samples without sand. The samples with the random Z seam had lower hoop stress then the samples tested with the regular Z seam. The samples in design 1 were twice as ductile as the samples in design 2.

Future Recommendations and OLC projects

The structural members in this research can be modified to further investigate the use of plastic to build structural members. Some of the modifications of the member that can be designed are as following:

1. Investigation of aging effects on 3D printed members.
2. Investigate how the compressive properties change when changing the infill parameters of the print. Being able to come up with an infill that is both strong and optimal is crucial in being economical.
3. Testing the samples on a large scale. To see if the size influences the different stresses acting on the member.
4. Exposing the members to extreme temperature differences as the structural members in the real world experience a variety of temperature changes throughout.
5. Investigate how different relative compaction percentages affect the properties of the structural members.

References

Davachi, S.M. and Kaffashi, B. (2015) *Polymer-Plastics Tech. & Eng.*, Vol. 54, 9, pp 944-967

Failure Analysis. (n.d.). Retrieved from http://www.engr.sjsu.edu/~WofMate/SanBruno/WebPipelineFailure.htm

The Free Beginner's Guide - 3D Printing Industry. (2018, April 20). Retrieved from https://3dprintingindustry.com/3d-printing-basics-free-beginners-guide#02-history

Gross, B. C., Erkal, J. L., Lockwood, S. Y., Chen, C., & Spence, D. M. (2014). Evaluation of 3D Printing and Its Potential Impact on Biotechnology and the Chemical Sciences. *Analytical Chemistry*, *86*(7), 3240-3253. doi:10.1021/ac403397r

History of 3D Printing: It's Older Than You Think. (2018, April 13). Retrieved from https://www.autodesk.com/redshift/history-of-3d-printing/

PLA Fibers. (2015). Retrieved from http://polymerdatabase.com/Fibers/PLA.html

Subel, M. (n.d.). P Patel. Retrieved from http://librarycivil.blogspot.com/2016/06/thin-cylinders.html

Stereolithography: 3D Printing by Laser solidyfing Liquid-Resin. (n.d.). Retrieved from https://www.sculpteo.com/en/glossary/stereolithography-definition/

MTS 370 Landmark. (n.d.). Retrieved from https://www.sdstate.edu/mts-370-landmark

Appendix A: Equations

$$D_r = \frac{e_{max} - e}{e_{max} - e_{min}} \times 100$$ Equation 3.1

$$e = \frac{V_V}{V_S}$$ Equation 3.2

$$V_V = V_T - V_S$$ Equation 3.3

$$V_S = \frac{M_S}{G_S \times \rho_w}$$ Equation 3.4

$$p = \frac{F}{A}$$ Equation 3.5

$$\sigma_l = \frac{p \times d_i}{2 \times t}$$ Equation 3.6

$$\sigma_c = \frac{p \times d_i}{t}$$ Equation 3.7

$$s = \sqrt{\frac{(\sum x^2 - nX^2)}{n-1}}$$ Equation 3.8